ADVANCED MATERIALS

Supporting Information

for *Adv. Mater.,* DOI: 10.1002/adma.201504045

Solution-Grown Silver Nanowire Ordered Arrays as Transparent Electrodes

*Beniamino Sciacca, Jorik van de Groep, Albert Polman, and Erik C. Garnett**

Supporting Information

Solution-grown Silver Nanowire Ordered Arrays as Transparent Electrodes

*Beniamino Sciacca, Jorik van de Groep, Albert Polman, and Erik C. Garnett**

On the use of a figure of merit to compare transparent electrodes

As mentioned in the manuscript the relative performance of transparent electrodes having different geometry, T and R_{sh} strongly depends on the technological application.[1] Using a single number (or figure of merit) can be highly deceiving, as this number can be made **arbitrarily** large. As an example, consider a metal grid with 100×100 nm nanowire cross-sections and 1000 nm pitch; by increasing both the size of the metal and of the pitch by a factor of 10, an electrode with 10-fold better sheet resistance and equal transmittance would be obtained. However, this could translate to much better or much worse solar cell performance depending on the carrier diffusion length and current being generated by the cell.

Correct description of transmittance of a thin metal film at low frequency

A *figure of merit*, defined as the ratio between dc conductivity to optical conductivity,[2-6] is widely used to link T to R_{sh}, and to compare different transparent electrodes. However we raise some concerns (i) on its applicability in the optical frequency regime and (ii) on the validity of the description.

First, a simple dependence of T to R_{sh} (Equation S1), similar to the widely employed figure of merit, can be obtained for a thin metal film in air only in the low frequency regime (ref [7] p. 363, Equation B.17):

$$T \approx \left(1+\frac{2\pi\sigma_{dc}d}{c}\right)^{-2} = \left(1+\frac{Z_0}{2R_{Sh}}\right)^{-2} \qquad \text{(S1)}$$

Where σ_{dc} is the dc conductivity, *d* the film thickness, *c* the speed of light, Z_0 is the free space impedance, and R_{sh} the sheet resistance. This approximation is only valid at low frequency, at which the imaginary part of the dielectric constant is much larger than the real part. Therefore Equation S1 is not valid for metals at optical frequencies, where the relation between T and R_{sh} becomes more complicated, and involves both the real and the imaginary part of the dielectric function.[7]

Second, note that in Equation S1 T is wavelength independent, and does not contain information about optical conductivity, whereas in the description first reported in [3] and then widely spread [2-6], σ_{dc} is substituted with σ_{ac}, the optical conductivity. This led to the appearance of the ratio σ_{ac}/σ_{dc}, which was then employed in the literature as a figure of merit, but it is an artifact lacking of any physical meaning. Only in the limiting case of $\sigma_{ac}=\sigma_{dc}$, the relationship between T and R_{sh} widely employed in literature[2-6] is correct and equals Equation S1, which is valid only in the low frequency regime.

Therefore we believe the widely used figure of merit doesn't have a physical meaning and should no longer be used to compare transparent electrodes.

Mayadas and Shatzkes' model.

$$\alpha = \frac{l_0}{d}\frac{R}{1-R} \tag{S2a}$$

$$f(\alpha) = 3\left[\frac{1}{3} - \frac{1}{2}\alpha + \alpha^2 - \alpha^3 \ln\left(1 + \frac{1}{\alpha}\right)\right] \tag{S2b}$$

$$g(k,p,\alpha) = \frac{6(1-p)}{\pi k}\int_0^{\pi/2} d\phi \int_0^{\pi/2} \frac{\cos(\vartheta)\sin^3(\phi)\cos^2(\phi)}{H^2}\,\frac{1-e^{-kH/\cos(\vartheta)}}{1-pe^{-kH/\cos(\vartheta)}}\,d\vartheta \tag{S2c}$$

$$H = 1 + \frac{\alpha}{\cos(\vartheta)\sin(\phi)} \tag{S2d}$$

$$k = \frac{t}{l_0} \tag{S2e}$$

$$\frac{\sigma_g}{\sigma_0} = \frac{1}{f(\alpha) - g(p,k,\alpha)} \tag{S2f}$$

Here, ϑ and ϕ are the angles in polar coordinates, t is the film thickness, l_0 is the electron mean free path (~58 nm for silver, calculated with the Drude model), d the average crystallite diameter, σ_g the conductivity of the polycrystalline sample, σ_0 the bulk conductivity, and $0<R<1$ a coefficient describing the likelihood for an electron to be reflected by a grain boundary (which is assumed to be perpendicular to the drift velocity). Losses due to electron scattering at the surface are taken into account in the specularity parameter $0<p<1$, with $p=0$ meaning diffuse scattering and $p=1$ specular scattering.

Nanowire network fabrication.

4-inch borosilicate wafers (0.7 mm thick) were cut and subsequently cleaned with base piranha. After a 2-5 min bake-out at 150 °C the samples were cooled with N_2. Next, ~250 nm Poly(methyl methacrylate) (mr-I PMMA, micro resist technology) 35 kDa (300) was spincoated at 1000 rpm in 45 s, followed by a 15 min bake at 150 °C. After cooling, the substrates were exposed to a 10 s O_2 plasma reactive-ion etch (RIE) to make the surface of the PMMA hydrophilic. Then, a 60 – 70 nm thick uniform layer of liquid silica sol-gel (details can be found in ref [8]) was spincoated at 1000 rpm (10 s), after which the nano-imprint stamp (containing multiple 2 × 2 mm nanopatterns) was applied. After 30 minutes of drying in ambient conditions, the stamp was removed and nanoscale trenches were formed in the solidified sol-gel layer. RIE was then used to anisotropically etch through the residual sol-gel layer (25 sccm CHF_3, 25 sccm Ar, 15 mTorr, 67 W, 1:45 min), followed by a 4 min O_2 plasma etch (25 sccm, 5 mTorr, 50 W) to etch through the PMMA layer and expose the glass substrate. Finally, another 6 min etch step (same CHF_3-based recipe as above) was performed to remove any residual sol-gel from the sample. This last step also etches shallow trenches into the glass substrate and leaves behind a clean PMMA template.

Metal deposition via solution phase.

The *reducing solution* was prepared by dissolving of D-glucose (6.84 g) in deionized water (20 mL). After complete dissolution of glucose, absolute methanol was added (10 mL). The *silver solution* was prepared by adding silver nitrate (0.815g) to deionized water (20 mL) and stirring at 400 rpm for 20 min. Potassium hydroxide (40 µL, 0.25 M) was added, producing a cloudy solution due to the precipitation of solid silver oxide particles (Ag_2O). Ammonium hydroxide (NH_4OH) (28-32%) was added drop wise until the solution became clear and transparent again, as a result of the formation of diamminesilver(I) complex $(Ag(NH_3)_2)^+$. The amount of NH_4OH added was typically around 950 µL. After 5 min, the *reducing solution* (20 mL) was added to the *silver solution,* while vigorously stirring to ensure homogeneous mixing of the reagents. The resulting solution was quickly poured into a plastic petri-dish containing the nanopatterned glass substrate. The reaction time was controlled to produce nanowire networks with different heights. After the desired growth time, the sample was rinsed first in a 20:1 H_2O:NH_4OH solution for 30 s, to quench the reaction, and subsequently in deionized water.

Lift-off procedure.

The sample was first transferred into an aqueous solution containing Polyvinylpyrrolidone (PVP) (55 kDa, 0.2 M) for 1h, then rinsed in deionized water and dried. The sample was then placed in a 1:3 H_2O:Ethanol solution with PVP (0.2 M) at 65 ºC, while stirring at 500 rpm. The solution dissolved the PMMA template, while PVP ensured the encapsulation of Ag nanoparticles present on PMMA, to avoid irreversible adhesion to the glass substrate by Van der Waals forces, and affect the transmission properties of the electrode. After 2 h, the sample was sonicated for 30 s to remove any residual PMMA from the surface, rinsed in isopropanol and N_2 dried.

Contact fabrication.

Thick Ag contacts on either side of the nanowire networks were fabricated using UV-lithography. After 2 – 5 min bake-out at 100 °C, the samples were spincoated with a HMDS primer (4000 rpm, 32 s) to improve the adhesion of the photoresist. After a 1 min bake at 100 °C, the samples were cooled and a ~925 nm thick layer of negative-tone photoresist (ma-N 1410 micro resist technology) was spincoated at 1400 rpm in 32 s, followed by a 90 s bake at 100 °C. The samples were then exposed for 22.5 s at 20 mW (450 mJ) through a flexible mask (Selba) to create 125 µm × 2 mm large contacts that have 50 µm overlap with the nanowire networks. The exposed resist was developed by rinsing in ma-D 533S (micro resist technology) for 85 s to create an undercut, followed by extensive rinsing in deionized water to stop the development, and dried using N_2. Next, thermal evaporation was used to deposit a 5 nm Cr adhesion layer (0.3 Å/s) and 150 nm of Ag (2.0 Å /s). Finally, lift-off was performed by soaking the sample in acetone (53 °C) for 1 – 2 hours, followed by rinsing in isopropanol and blow drying.

Transmission measurements.

A white-light super-continuum laser (Fianium SC400-4), attenuated using the reflection of a glass slide and a ND 2.0 filter, was used to illuminate the substrates. A f = 40 mm lens (Thorlabs, AC254-040-B-ML) was used to weakly focus the light onto the nanowire networks. The samples were mounted in front of an integrating sphere (LabSphere) such that also the diffusely scattered light is collected. The transmitted light is collected by a multi-mode collection fiber (105 µm core, Thorlabs FG105ACU) and sent to a spectrograph (ACTON spectrapro 2300i) and CCD camera (Pixis 400, cooled to -70 °C). The measured spectral range was 430 – 930 nm. Each reported spectrum is the result of 100 accumulated spectra, each with a 250 ms integration time. To isolate the transmittance of the nanowire networks, the spectra were normalized to the transmission of a flat and clean reference glass wafer. This normalization procedure, often employed in the field of transparent electrodes, overestimates the transmittance by 8% absolute. Spectra collected in three different positions on each network were averaged to account for any spatial variation on the sample.

Haze measurements

A white-light supercontinuum laser (Fianium WL-SC-400-4), sent through an acousto-optical tunable filter (AOTF, Crystal Technologies, roughly 4 nm bandwidth) was used as the light source in the 450-900 nm range. An amplified Si photodetectors (PDA100A, Thorlabs), connected to Stanford Research Systems SR830 lock-in amplifiers, was used to measure the output signal. The transmission of the AOTF was digitally modulated at 20 kHz with a 50 percent duty cycle. The beam power was monitored by a separate photodetector to account for fluctuations in the laser power. A f = 30 cm lens was used to focus light on the sample. Direct transmission in the 2.5-90º range was measured by placing the detector at a distance of 11 cm from the sample. Total transmission (0-90º) was measured by placing the sample in a custom-built integrating sphere (LabSphere). To isolate the transmittance of the nanowire networks, the spectra were normalized to the transmission of a flat and clean reference glass wafer. Spectra collected in two different positions on each network were averaged to account for any spatial variation on the sample

Sheet resistance measurements.

Four-point-probe sheet resistance measurements were performed by applying a current in the range -0.1A:0.1A (external terminals) and measuring the voltage drop across the network with two different probes (internal terminals). All the terminals were on the big Ag photolithography pads. The sheet resistance for the square networks was calculated as the ratio of the two quantities.

XRD.

The average grain size can be estimated using the well-known Scherrer equation;[9]

$$L = \frac{K\lambda}{B\cos(\theta)} \quad . \tag{S3}$$

Here, L is the average crystallite diameter, K is the Scherrer constant (a typical value is 0.9), λ is the x-ray wavelength (λ = 0.154 nm for Cu Kα), B is the 2θ XRD FHWM peak (in radians) corrected for the instrumental broadening, and θ is the Bragg angle. The Bruker D2-phaser instrument was used to collect the XRD spectra, in the θ-2θ configuration. An acquisition time of 0.2 s per step was used and more than 100 spectra were averaged to increase signal to noise ratio. The B values were obtained after correcting for instrumental intrinsic broadening;

this was done by measuring XRD of a Corundum standard sample and subtracting the FHWM of the peak at $2\theta = 35.1^{\circ}$, from the FHWM of the (111) reflection ($2\theta = 38.4^{\circ}$) in the Ag nanowire network sample.

RTA.

Rapid thermal annealing was performed in Sitesa addax RM6. The sample was placed on the silicon wafer susceptor, spaced by two 1 mm thick glass slides employed as insulator from the underlying substrate. The light source was turned on for a fixed amount of time (7s), and Ar (5 L/min) was flowed during the experiment up to 60 s after the exposure, to allow for cooling down without oxidation of the nanowires. The temperature setpoint was 600 ºC with a ramp rate of 250 ºC/s but the pyrometer never reached a stable value as it is not accurate below 600 ºC.

AFM.

Surface topographies were measured using a Digital Instruments Dimension 3100 atomic force microscope. 4×4 micron areas (384×384 pixels) were scanned using tapping mode (163.344 kHz tapping frequency) and a horizontal scan speed of 2 s/line. For Figure S2, a 10x10 micron area was scanned using tapping mode (140.48 kHz tapping frequency) and a horizontal scan speed of 5 s/line.

References

[1] M. W. Rowell, M. D. McGehee, *Energ Environ Sci* **2011**, 4, 131.
[2] S. De, T. M. Higgins, P. E. Lyons, E. M. Doherty, P. N. Nirmalraj, W. J. Blau, J. J. Boland, J. N. Coleman, *Acs Nano* **2009**, 3, 1767.
[3] L. Hu, D. S. Hecht, G. Gruner, *Nano Lett* **2004**, 4, 2513.
[4] L. B. Hu, H. Wu, Y. Cui, *Mrs Bull* **2011**, 36, 760.
[5] B. Han, K. Pei, Y. L. Huang, X. J. Zhang, Q. K. Rong, Q. G. Lin, Y. F. Guo, T. Y. Sun, C. F. Guo, D. Carnahan, M. Giersig, Y. Wang, J. W. Gao, Z. F. Ren, K. Kempa, *Adv Mater* **2014**, 26, 873.
[6] J. V. van de Groep, P. Spinelli, A. Polman, *Nano Lett* **2012**, 12, 3138.
[7] M. Dressel, G. Gruner, *Electrodynamics of Solids: Optical Properties of Electrons in Matter*, Cambridge University Press, Cambridge 2002.
[8] J. van de Groep, P. Spinelli, A. Polman, *Nano Lett* **2015**, 15, 4223.
[9] B. Fultz, J. M. Howe, *Transmission Electron Microscopy and Diffractometry of Materials*, Springer, 2000.
[10] S. R. Ye, A. R. Rathmell, Z. F. Chen, I. E. Stewart, B. J. Wiley, *Adv Mater* **2014**, 26, 6670.
[11] C. Preston, Y. L. Xu, X. G. Han, J. N. Munday, L. B. Hu, *Nano Res* **2013**, 6, 461.

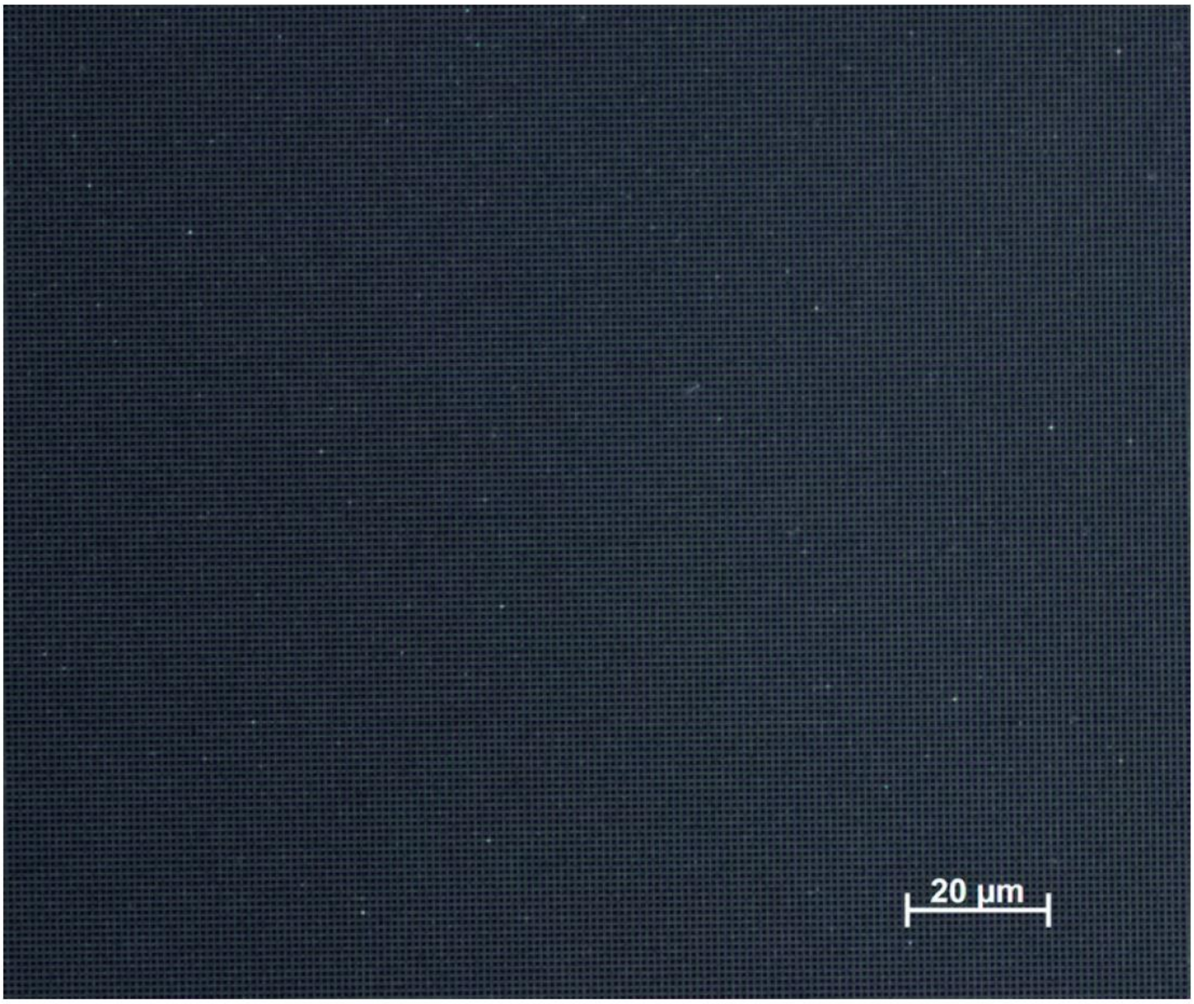

Figure S1: Optical image of Ag nanowire networks. The pitch of the array is 1000 nm.

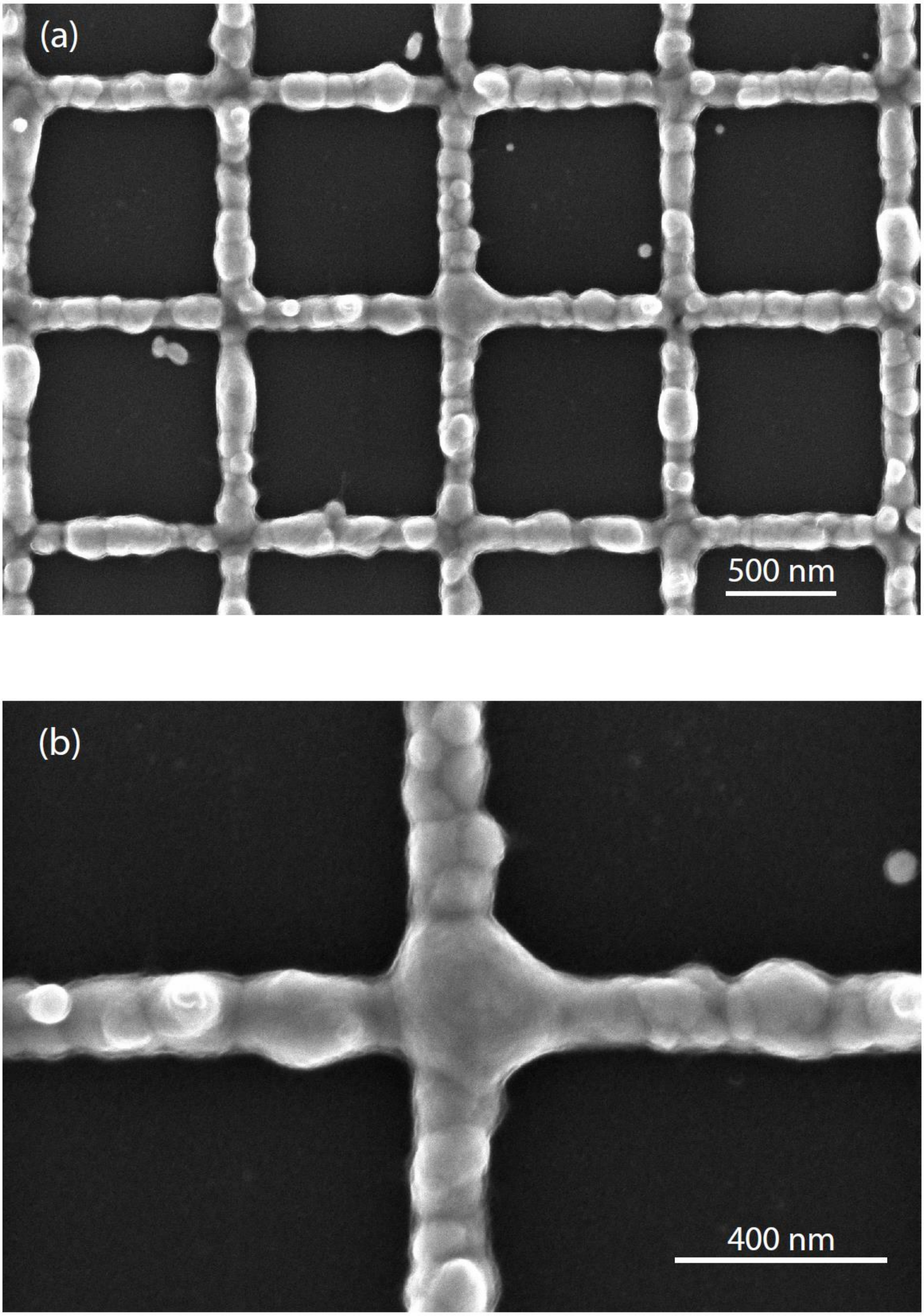

Figure S2: (a) High resolution SEM image of a solution processed Ag nanowire network. (b) High magnification detail of (a).

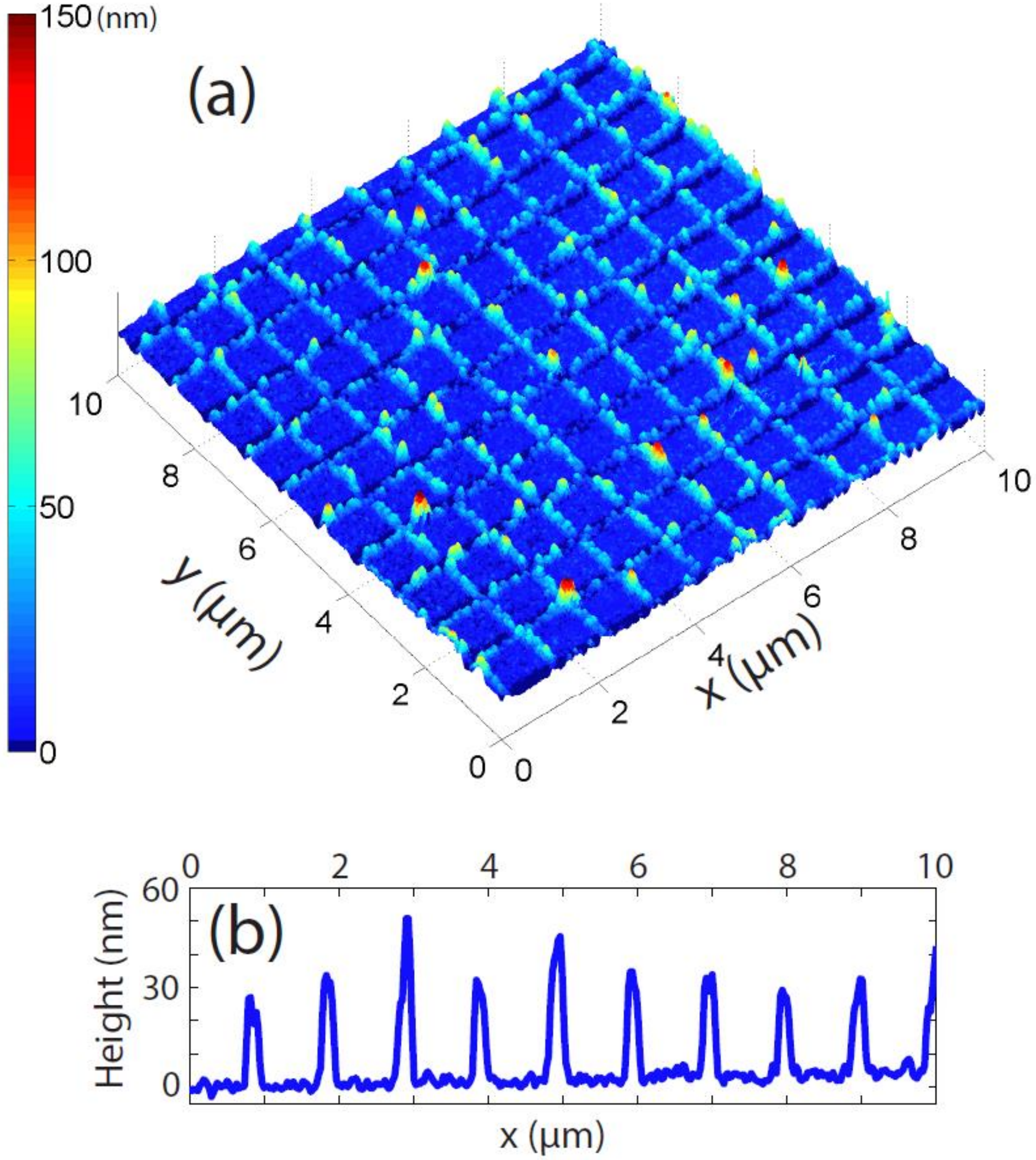

Figure S3: (a) 10x10 µm AFM scan of Ag nanowire networks. (b) Cross-cut of the image.

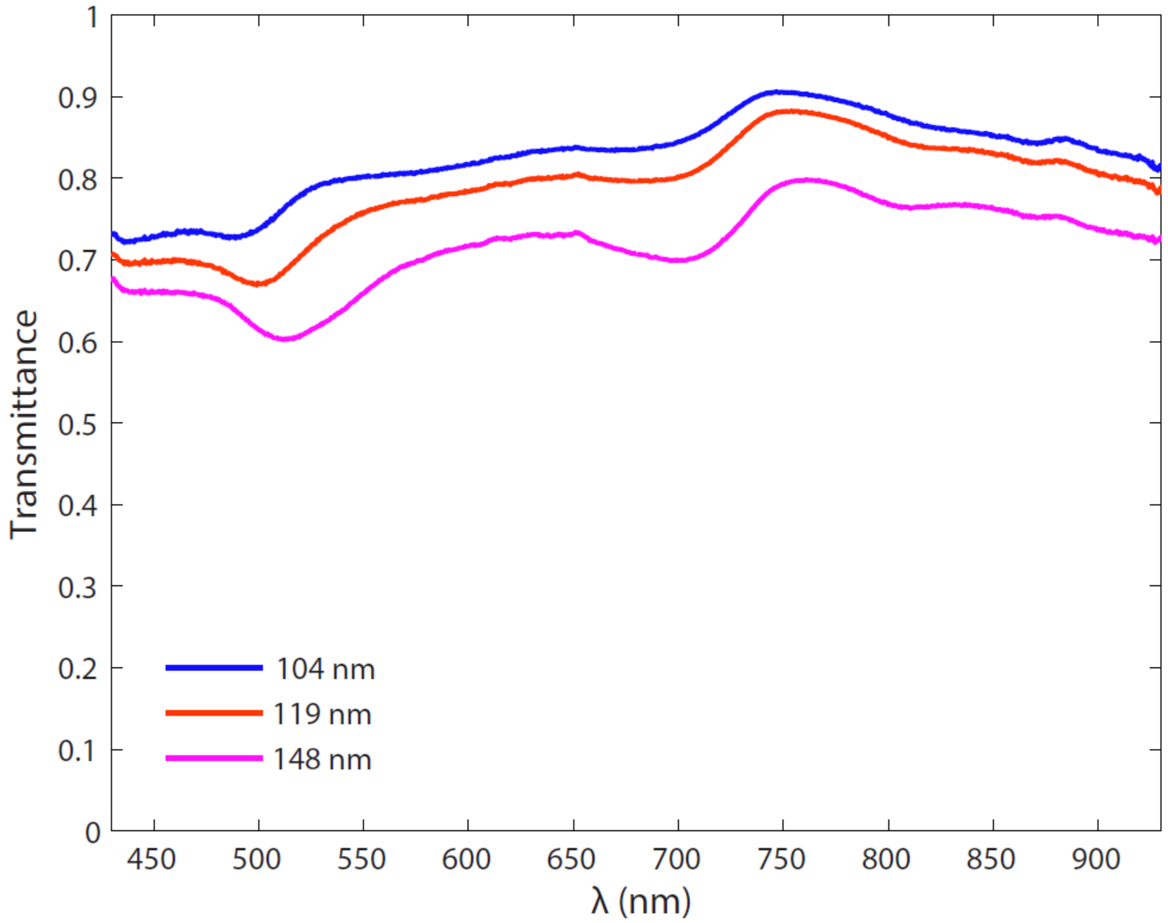

Figure S4: Transmittance of solution-grown nanowire networks with an average height of 30 nm, normalized to the glass substrate; the different curves correspond to different nanowire widths; the pitch is 1000 nm.

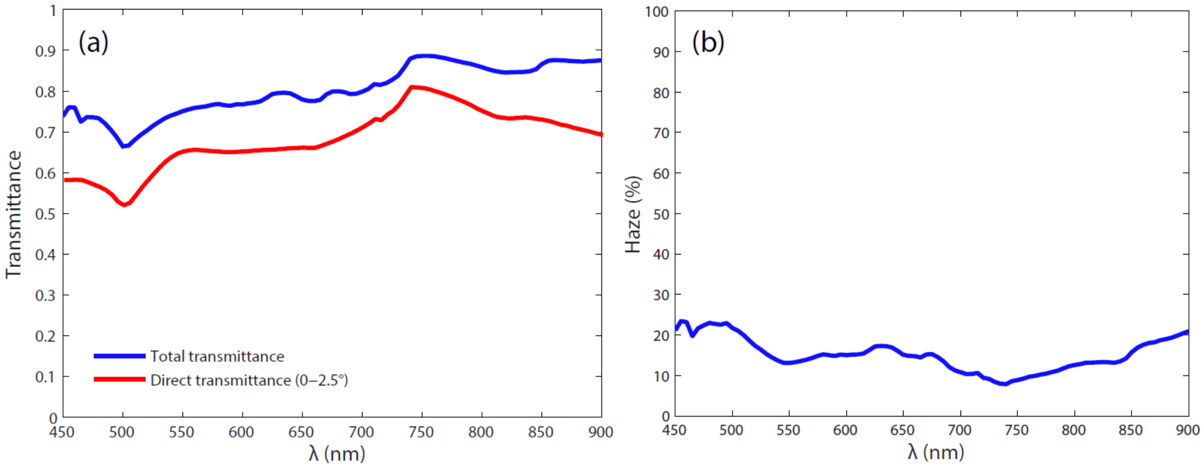

Figure S5: (a) Total transmittance (0-90°) and direct transmittance (0- 2.5°) for a solution processed silver nanowire network, with 1000 nm pitch. (b) Haze as a function of wavelength calculated from (a) as the ratio between forward scattered light in the 2.5-90º range, to total transmitted light (0-90º). An integrated haze value of 14.9% was obtained by weighting (b) for the AM1.5 spectrum in the range 450-900 nm. Note that one of the advantages of our controlled geometry is that the light-matter interactions (including haze) can be engineered to fit a given application.[10, 11]

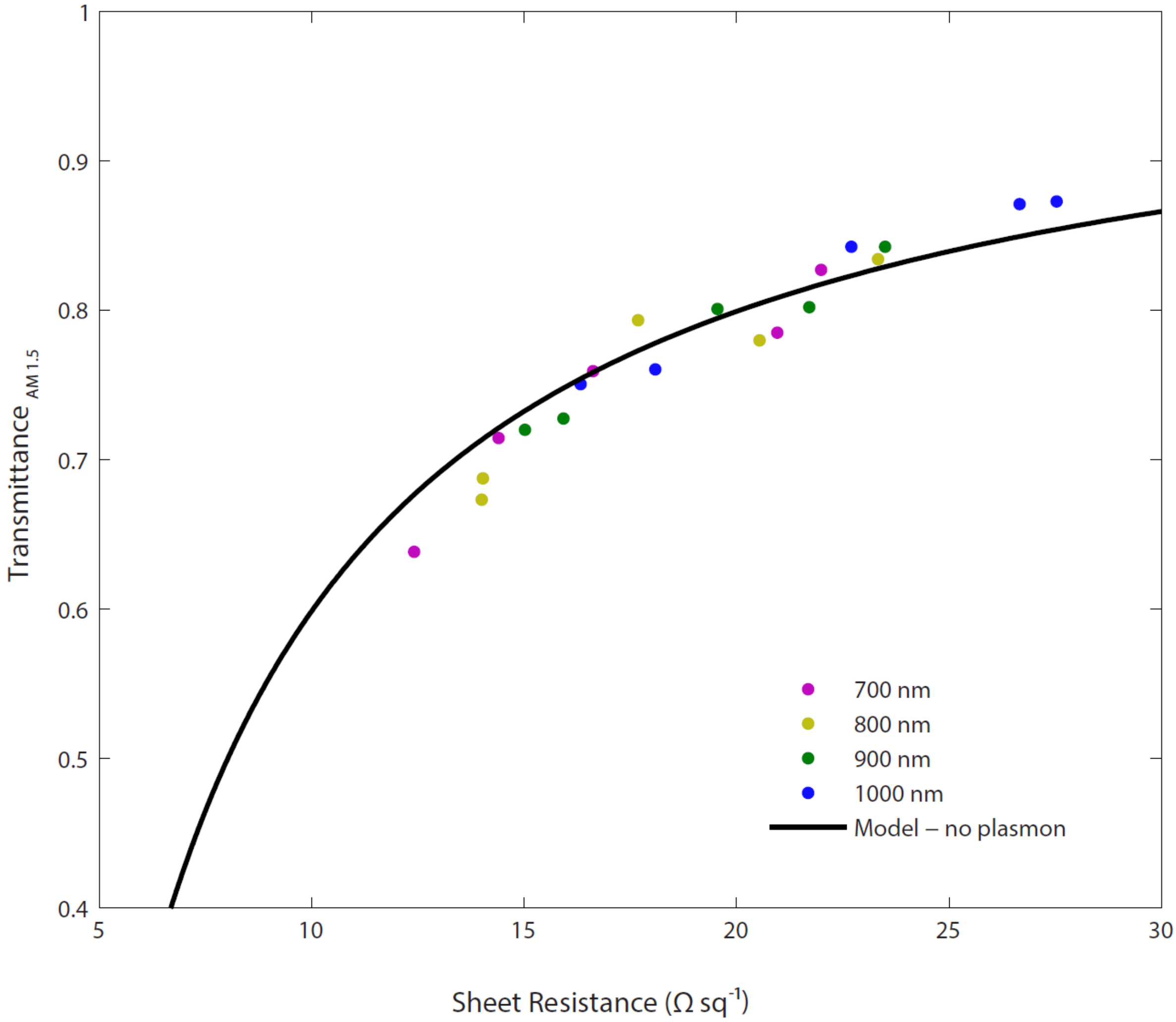

Figure S6. Optical vs electrical performance of evaporated Ag nanowire networks with a thickness of 30 nm for different nanowire width; the different colors represent a different pitch of the array. The solid black curve represents the theoretical performance of 30 nm thick nanowire networks of various pitch/width ratio; the sheet resistance is calculated from the Mayadas-Shatzkes model (p=0.5, R=0.57, d=15nm) and the transmittance is calculated by adding the transmission through voids and the wavelength dependent transmission through the 30 nm metal film (weighted for the AM1.5 spectrum); plasmonic effects are not taken into account. This shows that this simple model describes well the experimental data.